Abiogenic Methane Formation and Isotopic Fractionation Under Hydrothermal Conditions

Juske Horita[1]* and Michael E. Berndt[2]

Recently, methane (CH_4) of possible abiogenic origin has been reported from many localities within Earth's crust. However, little is known about the mechanisms of abiogenic methane formation, or about isotopic fractionation during such processes. Here, a hydrothermally formed nickel-iron alloy was shown to catalyze the otherwise prohibitively slow formation of abiogenic CH_4 from dissolved bicarbonate (HCO_3^-) under hydrothermal conditions. Isotopic fractionation by the catalyst resulted in $\delta^{13}C$ values of the CH_4 formed that are as low as those typically observed for microbial methane, with similarly high $CH_4/(C_2H_6 + C_3H_8)$ ratios. These results, combined with the increasing recognition of nickel-iron alloy occurrence in oceanic crusts, suggest that abiogenic methane may be more widespread than previously thought.

Methane, by far the most abundant natural gas, is formed largely by the digestion of organic compounds by microorganisms (microbial origin) and the thermal decomposition of organic matter (thermogenic origin). Although the occurrence of deep-Earth, mantle methane is still controversial (*1, 2*), reports of high-temperature fluids venting from sediment-poor mid-ocean ridges (*3*), seepages from regions associated with ultramafic rocks on land (*4*), fluids from Precambrian shields (*5*), and fluid inclusions in mantle and igneous rocks (*6*) suggest the inorganic (abiogenic) formation of methane in Earth's crust. Several geochemical indicators have been used to distinguish methane of different origins, primarily between microbial and thermogenic. Primary criteria applied to date include $CH_4/(C_2H_6 + C_3H_8)$ ratios and carbon and hydrogen isotope compositions of methane (*7*). However, there are very few indicators or criteria for distinguishing methane of abiogenic origin (*8*); the occurrence of unambiguously abiogenic methane has been documented on only a few occasions, and very little is known about the natural processes that produce it.

It is recognized that abiogenic methane formation is prohibitively slow in the absence of catalysts at low to moderately high temperatures even under reducing conditions, where methane is thermodynamically the most stable carbon-bearing form. However, recent experiments (*9*) demonstrated that dissolved HCO_3^- can be converted to CH_4 and other hydrocarbons in the presence of ultramafic rocks under reducing hydrothermal conditions; this suggests that natural minerals with high iron or other transition metal content can catalyze the formation of abiogenic CH_4. If this process is widely operative in nature, abiogenic methane could be more widespread than previously thought. Determining isotopic fractionation during abiogenic CH_4 formation is of particular importance because isotopic composition is widely used as a tool for identifying the origin and mechanisms of CH_4 formation. Here, we report experimental results on isotopic fractionation of CH_4 abiotically formed from dissolved HCO_3^- under hydrothermal conditions.

Experiments were performed under conditions similar to those commonly encountered during the serpentinization of ultramafic rocks of the oceanic crust (temperatures of ≤400°C and pressures of ≤100 MPa), where olivine is converted to serpentine and magnetite, producing H_2, while released Ni is deposited as awaruite (Ni_3Fe). First, a mixture of magnetite and Ni-Fe alloy in an H_2-rich aqueous solution (250 to 300 mmol/kg soln) was generated at 400°C and 50 MPa inside a closed, flexible gold-cell hydrothermal apparatus (*10*). After cooling the vessel to the study conditions, a $NaHCO_3$ solution was injected once to reach an initial total dissolved carbonate species (ΣCO_2) (*11*) of about 5 to 12 mmol/kg soln in the fluid. Samples were then collected periodically for analysis of dissolved gases to monitor CH_4 formation (*12*). A series of experiments was conducted at 200° to 400°C and 50 MPa, including two in which isotopic fractionation was measured (*13*). Methane formed rapidly in the presence of the Ni-Fe alloy (Fig. 1) via the reaction

$$HCO_3^- + 4H_2 \rightarrow CH_4 + OH^- + 2H_2O \quad (1)$$

In a control experiment where no Ni-Fe alloy was present at 400°C, no methane was formed (Fig. 1C). The amounts of methane produced were directly related to the amount of Ni-Fe alloy (8 to 49 mg in ~46 g of water). These observations indicate that methane formation from HCO_3^- is catalyzed by the Ni-Fe alloy, not by magnetite. Reaction at 400°C appeared to slow markedly with time, whereas reaction at 300°C was much faster and continued to near completion. An experiment at 200°C required even longer reaction times.

The combined concentrations of ΣCO_2 and CH_4 in the fluid decreased early in the experiments, but rebounded toward the end of each experiment. This indicated the presence of an intermediate carbon phase or species during the reduction of HCO_3^- to CH_4. Thus, the overall reaction described by Eq. 1 is better described by a chain reaction via an intermediate product or products, $HCO_3^- \rightarrow$ intermediate(s) $\rightarrow CH_4$. Intermediate products such as carbon monoxide (CO), graphitic carbon, and carbide phases are commonly found in dry-gas CO_2 methanation, although the precise role that each plays in the reactions is not always clearly understood (*14*). No CO was detected in the fluids during the experiments, and no carbon phases were detected in the solids after the

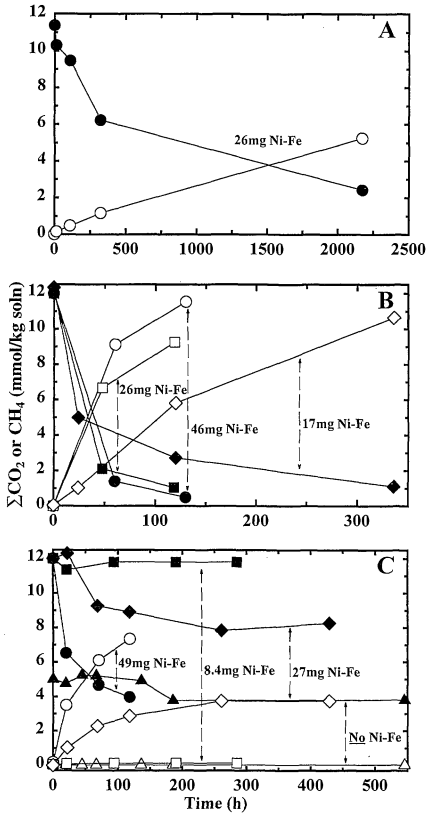

Fig. 1. Chemical composition of fluids during abiogenic hydrothermal CH_4 (open symbols) formation from total dissolved CO_2 (ΣCO_2, closed symbols) in water (~46 g) for (**A**) 200°C and 50 MPa with 26 mg of Ni-Fe alloy, (**B**) 300°C and 50 MPa with 17 mg (diamonds), 26 mg (squares), and 46 mg (circles) of Ni-Fe alloy, and (**C**) 400°C and 50 MPa with 0 mg (triangles), 8.4 mg (squares), 27 mg (diamonds), and 49 mg (circles) of Ni-Fe alloy. HCO_3^- was a predominant (>70%) CO_2 species in the fluids.

[1]Chemical and Analytical Sciences Division, Oak Ridge National Laboratory, Oak Ridge, TN 37831, USA. [2]Department of Geology and Geophysics, University of Minnesota, Minneapolis, MN 55455, USA.

*To whom correspondence should be addressed. E-mail: horitaj@ornl.gov

experiments had been completed (*10*). One possibility for the intermediate species in the experiments is formate ion ($HCOO^-$), because formate, a hydrated form of CO, is thermodynamically more stable than CO under hydrothermal conditions (*15*). This species could not have been detected by the gas chromatography techniques used here (*12*), but it was observed as a common intermediate product in similar experiments using ion chromatography techniques at 200° to 300°C (*16*). However, because we did not measure formate concentrations in our Ni-Fe alloy experiments in Fig. 1, and because we cannot rule out the existence of other intermediate species, the concentration of the intermediate product or products was calculated as a single component using mass balance constraints (Table 1). The fact that this intermediate phase was present early in the experiments suggests that it forms from dissolved CO_2 more rapidly than it is converted to CH_4.

In the two isotope experiments, the $\delta^{13}C$ value of ΣCO_2 steadily increased while HCO_3^- was reduced (Fig. 2). The $\delta^{13}C$ values of the CH_4 produced, on the other hand, were consistently much lower than those of ΣCO_2, and increased slightly with reaction progress. The $\delta^{13}C$ values of the intermediate product, calculated from an isotope mass balance of the system, were initially between those of ΣCO_2 and CH_4 at 200°C. However, at the end of the experiment, the calculated $\delta^{13}C$ value of the intermediate product became higher than that of the residual ΣCO_2 (Fig. 2A). At 300°C, the $\delta^{13}C$ value of the intermediate product was only slightly lower than that of ΣCO_2 by the time the first sample was collected, but much higher than that of CH_4. The $\delta^{13}C$ value of the intermediate eventually surpassed that of the coexisting ΣCO_2 (Fig. 2B).

Overall $^{13}C/^{12}C$ isotope fractionation during

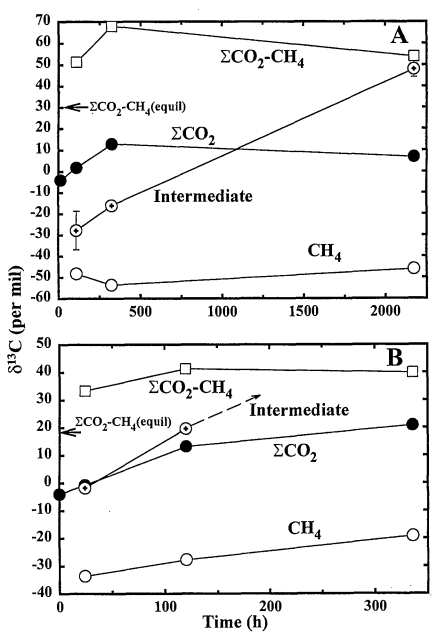

Fig. 2. $\delta^{13}C$ values of fluids during abiogenic hydrothermal CH_4 formation from total dissolved CO_2 (ΣCO_2) in water for (**A**) 200°C and 50 MPa with 26 mg of Ni-Fe, and (**B**) 300°C and 50 MPa with 17 mg of Ni-Fe. The $\delta^{13}C$ values of intermediate products were calculated from an isotope mass balance (Table 1).

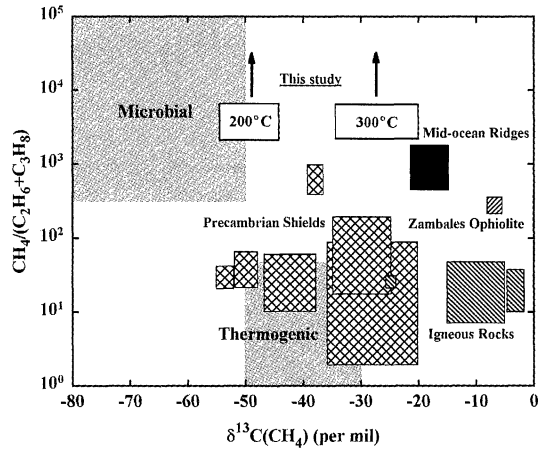

Fig. 3. Plot of $\delta^{13}C(CH_4)$ and $CH_4/(C_2H_6 + C_3H_8)$ values of abiogenic methane hydrothermally formed at 200° and 300°C and at 50 MPa in this study (open rectangles), together with values for biogenic (microbial and thermogenic) methane (*7*) and several reported values for abiogenic methane (*3–6*). $CH_4/(C_2H_6 + C_3H_8)$ ratios of abiogenic CH_4 in this study are lower limits, as shown by arrows, because both C_2H_6 and C_3H_8 were always below the detection limit (~1 μmol/kg soln). $\delta^{13}C$ values of ≥–25 per mil have been suggested for abiogenic CH_4 (*8*).

Table 1. Chemical and isotopic composition of fluids during abiogenic hydrothermal CH_4 formation from dissolved CO_2. Values for intermediates were calculated from carbon mass and isotope balances with propagated errors (1σ). For the dissolved gas concentrations, the overall analytical error is ±5%, except for the intermediate. Values of $\delta^{13}C$ are with respect to the Vienna Pee Dee belemnite standard, ±0.1 per mil for ΣCO_2 and ±0.5 per mil for CH_4.

Time (hours)	Chemical composition (mmol/kg soln)				Isotopic composition [$\delta^{13}C$ (per mil)]		
	ΣCO_2*	CH_4	Intermediate	H_2	ΣCO_2	CH_4	Intermediate
			200°C, 50 MPa (26 mg Ni-Fe)				
0	11.4	0	0	254	−4.1		
13.4	10.3	0.15	0.93 ± 0.51	173			
108.9	9.46	0.47	1.45 ± 0.47	239	1.7	−48.3	−27.8 ± 9.1
323.4	6.22	1.16	4.00 ± 0.31	233	12.9	−53.6	−16.1 ± 1.3
2173.4	2.42	5.25	3.72 ± 0.29	221	6.8	−46.0	48.0 ± 3.7
			300°C, 50 MPa (17 mg Ni-Fe)				
0	12.3	0.04	0	280	−4.1		
24.0	4.99	1.03	6.36 ± 0.25	271	−0.8	−33.6	−1.8 ± 0.1
120.0	2.72	5.81	3.85 ± 0.32	250	13.1	−27.8	19.6 ± 1.6
336.0	1.11	10.7	0.62 ± 0.53	230	20.8	−19.1	†
			300°C, 50 MPa (26 mg Ni-Fe)				
0	12.0	0	0	275			
47.5	2.1	6.67	3.23 ± 0.35	233			
118.5	1.05	9.25	1.7 ± 0.47	214			
			300°C, 50 MPa (46 mg Ni-Fe)				
0	12.0	0	0	297			
60.0	1.4	9.12	1.48 ± 0.46	220			
130.0	0.49	11.53	−0.02 ± 0.58	222			
			400°C, 50 MPa (8.4 mg Ni-Fe)				
0	12.0	0.04	0	260			
20.8	11.3	0.09	0.60 ± 0.57	268			
94.0	11.8	0.12	0.12 ± 0.59	266			
189.8	11.8	0.12	0.12 ± 0.59	265			
284.8	11.8	0.12	0.12 ± 0.59	246			
			400°C, 50 MPa (27 mg Ni-Fe)				
0	12.0	0	0	283			
21.8	12.3	1.02	−1.32 ± 0.62	270			
68.3	9.26	2.28	0.46 ± 0.48	261			
117.8	8.91	2.86	0.23 ± 0.47	262			
260.5	7.84	3.74	0.42 ± 0.43	254			
428.8	8.27	3.74	−0.01 ± 0.45	252			
			400°C, 50 MPa (49 mg Ni-Fe)				
0	12.0	0.17	0	218			
20.0	6.52	3.50	2.15 ± 0.37	204			
70.5	4.67	6.11	1.39 ± 0.38	184			
118.0	3.97	7.34	0.86 ± 0.42	196			

*ΣCO_2 = total dissolved carbonate species, dominated by HCO_3^- (>70%) (*11*). †Not shown because of large propagated error.

the formation of abiogenic CH_4 from dissolved CO_2 (largely HCO_3^-) was evaluated as $\alpha = (^{13}CH_4/^{12}CH_4)/(^{13}CO_2/^{12}CO_2) = 0.940$ to 0.950 (−50 to −60 per mil) at 200°C and $\alpha = 0.960$ to 0.965 (−35 to −40 per mil) at 300°C (Fig. 2). Equilibrium $^{13}C/^{12}C$ fractionations expected between ΣCO_2 and CH_4 in this study were calculated as α(equil) = 0.970 (−30 per mil) at 200°C and α(equil) = 0.982 (−18 per mil) at 300°C, with an uncertainty of ±5 per mil (*17*). The direction of isotope fractionation obtained from our experimental results is the same as those of the equilibrium fractionation factors, but their magnitudes are much larger. This suggests that the reduction of HCO_3^- via intermediate(s) to CH_4 was largely controlled by kinetic isotopic fractionation. The magnitude of overall kinetic isotope fractionations observed during abiogenic CH_4 formation from HCO_3^- under hydrothermal conditions is as large as those of microbial reduction of CO_2 to CH_4 by methanogenic bacteria at ambient temperature (α = 0.93 to 0.96) (*18*). There is, to our knowledge, no experimental study on carbon isotope fractionation during hydrothermal CH_4 formation from dissolved CO_2, although several studies of the conversion of CO to CH_4, CO_2, and other hydrocarbons in the presence of Co or Fe catalysts under dry H_2 atmosphere (Fischer-Tropsch reaction) showed large, variable kinetic carbon isotope fractionation (α = 0.94 to 0.99) (*19*).

Our experimental results show that abiogenic methane forms rapidly in the presence of even small amounts of hydrothermally generated Ni-Fe alloys under reducing conditions. In nature, Ni-Fe alloys are important phases in the paragenetic sequence of minerals that form during hydrothermal alteration of olivine-rich rocks (*20*). Olivine commonly contains several thousand parts per million of Ni, and it commonly converts to Ni-Fe alloys under the reducing conditions that typically prevail during serpentinization. Awaruite, Ni-Fe alloy, and Ni-Fe sulfide have been reported from many continental ultramafic settings (*20*), oceanic crustal environments (*21*), and meteorites (*22*). Indeed, the oceanic crust is largely composed of ultramafic rocks, and serpentinite containing awaruite and Ni-Fe alloy could make up a large fraction of the oceanic crust (*23*). Thus, abiogenic methane formation via an awaruite/Ni-Fe alloy–catalyzed reaction may occur more commonly in Earth's crust than is currently recognized.

As noted above, the criteria for identifying methane as abiogenic are very ambiguous (*7, 8*). One suggested geochemical criterion is $\delta^{13}C$ values higher than −25 per mil, based on limited isotopic data of probable abiogenic CH_4 (Fig. 3) (*8*). However, our experimental results reveal that $\delta^{13}C$ values of abiogenic CH_4 formed from dissolved CO_2 with a mantle-like $\delta^{13}C$ value (−4 per mil) can be very low, and may overlap values typical for microbial CH_4 (Fig. 3). Moreover, the high $CH_4/(C_2H_6 + C_3H_8)$ ratios of the gases produced by the Ni-Fe alloy are also similar to those of microbial origin. This is in direct contrast to previous results, where abiogenic methane formation catalyzed by magnetite was accompanied by ethane and propane (*9*). The chemical compositions of abiogenic hydrocarbon gases clearly depend strongly on the catalysts and mechanisms involved (*14*). This may explain low $CH_4/(C_2H_6 + C_3H_8)$ ratios of probable abiogenic methane found in many localities (Fig. 3). Another suggested criterion for abiogenic CH_4 is that $\delta^{13}C$ value decreases in the order CH_4, C_2H_6, and C_3H_8 ("isotopic reversal") (*8*). However, limited experimental data (*19*) suggest that this is not necessarily the case for abiogenic hydrocarbons. It has been suggested that reduced carbonaceous materials from early Archaean sediments, which have low $\delta^{13}C$ values (≤−20 per mil), are of biogenic origin (*24*). However, our results show that kinetic isotopic fractionation during abiotic processes can also produce reduced carbon-bearing species with very low $\delta^{13}C$ values.

The demonstrated hydrothermal synthesis of organic compounds (organic acids, hydrocarbons, alcohols) (*25*) under conditions resembling those in Earth's upper crust may have implications for the possible abiogenic formation not only of methane, but also of petroleum (*26*) and for the evolution of prebiotic organic molecules in the early oceans (*27*).

References and Notes

1. T. Gold, *J. Pet. Geol.* **1**, 3 (1979).
2. _____, in *The Future of Energy Gases*, D. Howell, Ed. (U.S. Geological Survey Professional Paper 1570), pp. 57–82 (1993).
3. P. A. Rona *et al.*, *Geology* **20**, 783 (1992); J. L. Charlou and J. P. Donval, *J. Geophys. Res.* **98**, 9625 (1993); J. L. Charlou *et al.*, *ibid.* **101**, 15899 (1996); J. A. Welhan, *Chem. Geol.* **71**, 183 (1988).
4. T. A. Abrajano *et al.*, *Chem. Geol.* **71**, 211 (1988); T. A. Abrajano *et al.*, *Appl. Geochem.* **5**, 625 (1990).
5. B. Sherwood *et al.*, *Chem. Geol.* **71**, 223 (1988); B. Sherwood Lollar *et al.*, *Geochim. Cosmochim. Acta* **57**, 5087 (1993); A. W. A. Jeffrey and I. R. Kaplan, *Chem. Geol.* **71**, 237 (1988).
6. D. S. Kelley, *J. Geophys. Res.* **101**, 2943 (1996); _____ and G. Frueh-Green, *Eos* **76**, F675 (1995); I. A. Petersil'ye and V. A. Pripachkin, *Geochem. Int.* **16** (no. 4), 50 (1979); J. Konnerup-Madsen, R. Kreulen, J. Rose-Hansen, *Bull. Mineral.* **111**, 567 (1988); J. Potter *et al.*, *Eur. J. Mineral.* **10**, 1167 (1998); E. M. Galimov, *NASA TT F-682* (1975).
7. M. Shoell, *Chem. Geol.* **71**, 1 (1988); M. J. Whiticar, *Org. Geochem.* **16**, 531 (1990).
8. P. D. Jenden, D. R. Hilton, I. R. Kaplan, H. Craig, in (*2*), pp. 31–56.
9. D. R. Janecky and W. E. Seyfried Jr., *Geochim. Cosmochim. Acta* **50**, 1357 (1986); M. E. Berndt, D. E. Allen, W. E. Seyfried Jr., *Geology* **24**, 351 (1996); D. E. Allen, M. E. Berndt, W. E. Seyfried Jr., J. Horita, *Eos* **79**, F58 (1998).
10. Powdered pure Fe metal (~0.5 g) and NiO (≤0.06 g) were reacted with deionized water (~46 g) in a closed gold bag at 400°C and 50 MPa to produce magnetite and Ni-Fe alloy, via the reactions $3Fe + 4H_2O \rightarrow Fe_3O_4 + 4H_2$ and $xNiO + yFe + xH_2 \rightarrow Ni_xFe_y + xH_2O$. The reaction reached completion within 5 days, as monitored by H_2 concentration. X-ray diffraction identified a small peak (d = 2.03 to 2.04 Å) characteristic for a Ni-Fe alloy with the awaruite structure (X_{Fe} = 0.02 to 0.10), disseminated within a matrix of magnetite grains. Scanning electron spectroscopy showed that the Ni-Fe alloy was porous and had a similar texture in all experiments. Extensive micrometer-scale mapping of the solid phase, using an electron microprobe with a wavelength-dispersive detector, revealed no carbon phase.
11. $\Sigma CO_2 = CO_2(aq) + H_2CO_3 + HCO_3^- + CO_3^{2-}$. HCO_3^- was predominant (>70%) in the fluids in all experiments, as calculated with SUPCRT92 [J. W. Johnson, E. H. Oelkers, H. C. Helgeson, *Comp. Geosci.* **18**, 899 (1992)].
12. Dissolved gases (CO, CO_2, H_2, CH_4, C_2H_6, and C_3H_8) in fluid samples were extracted and measured at the University of Minnesota by gas chromatography equipped with methanizer and thermal conductivity–flame ionization detectors. Overall analytical error, including the sampling procedure, is about ±5%. C_2H_6 and C_3H_8 were always below detection limit (~1 μmol/kg soln).
13. Fluid samples for isotope analysis were collected into a gas-tight Teflon syringe and transferred to Oak Ridge National Laboratory. A gas phase (mainly H_2 and CH_4) was injected into a vacuum line through a rubber septum. Small amounts of water and CO_2 were separated cryogenically from H_2 and CH_4. The CH_4 was finally converted to CO_2 with CuO at 800°C. Total dissolved carbonate, dominantly in the form of HCO_3^-, in the water samples was quantitatively recovered by acidifying them in vacuum with H_3PO_4.
14. A. M. Gadalla and B. Bower, *Chem. Eng. Sci.* **43**, 3049 (1988); T. Kai, T. Takahashi, S. Furusaki, *Can. J. Chem. Eng.* **66**, 343 (1988); M. D. Lee, J. F. Lee, C. S. Chang, *J. Chem. Eng. Jpn.* **23**, 130 (1990); C. N. Satterfield, R. T. Hanlon, S. E. Tung, Z. Zou, G. C. Papaefthymlou, *Ind. Eng. Chem. Prod. Res. Dev.* **25**, 401 (1986); *ibid.*, p. 407; V. C. H. Kroll, H. M. Swaan, S. Lacombe, C. Mirodatos, *J. Catal.* **164**, 387 (1997); G. D. Weatherbee and C. H. Bartholomew, *ibid.* **77**, 460 (1982).
15. E. L. Shock, *Geochim. Cosmochim. Acta* **57**, 3341 (1993).
16. J. Horita and M. E. Berndt, data not shown.
17. Large isotopic differences exist among different dissolved CO_2 species in the fluid [$CO_2(aq)$, HCO_3^-, and CO_3^{2-}] [S. Halas, J. Szaran, H. Niezgoda, *Geochim. Cosmochim. Acta* **61**, 2691 (1997); S. D. Malinin, O. I. Kropotova, V. A. Grinenko, *Geochem. Int.* **4**, 764 (1967)]. The calculations took these different dissolved CO_2 species into account and used partition function ratios of CO_2 and CH_4 [P. Richet, Y. Bottinga, M. Javoy, *Annu. Rev. Earth Planet. Sci.* **5**, 65 (1977)]. Isotope fractionations between gaseous and dissolved forms of CO_2 and CH_4 were neglected.
18. R. Botz, H.-D. Pokojski, M. Schmitt, M. Thomm, *Org. Geochem.* **25**, 255 (1996).
19. M. S. Lancet and E. Anders, *Science* **170**, 980 (1970); G. U. Yuen *et al.*, *Lunar Planet. Sci.* **XXI**, 1367 (1990); G. Hu, Z. Ouyang, X. Wang, Q. Wen, *Sci. China* **41**, 202 (1998).
20. J. B. Moody, *Can. Mineral.* **14**, 462 (1976); B. R. Frost, *J. Petrol.* **26**, 31 (1985).
21. J. C. Alt and W. C. Shanks III, *J. Geophys. Res.* **103**, 9917 (1998).
22. A. N. Krot *et al.*, *Geochim. Cosmochim. Acta* **61**, 219 (1997).
23. J. E. Snow, *Nature* **374**, 413 (1995).
24. S. J. Mojzsis *et al.*, *ibid.* **384**, 55 (1996); M. T. Rosing, *Science* **283**, 674 (1999).
25. M. Azuma, K. Hashimoto, M. Watanabe, T. Sakata, *J. Electroanal. Chem.* **294**, 299 (1990); C. Huber and G. Wächtershäuser, *Science* **276**, 245 (1997).
26. P. Szatmari, *Am. Assoc. Petrol. Geol. Bull.* **73**, 989 (1989).
27. E. L. Shock, *Orig. Life Evol. Biosp.* **20**, 331 (1990).

28. We thank D. Cole, B. Seyfried, and D. Allen for discussion and comments, and R. Knurr for analytical support. Sponsored by the U.S. Department of Energy Geosciences Program under contract DE-AC05-96OR22464 with Oak Ridge National Laboratory, managed by Lockheed Martin Energy Research Corp., and NSF grant OCE-9402507 to the University of Minnesota.

7 May 1999; accepted 15 June 1999